

---

# SCALING FOUNDATION MODELS FOR RADAR SCENE UNDERSTANDING

---

**Pushkal Mishra**

University of California San Diego  
pumishra@ucsd.edu

**Kshitiz Bansal**

Blue River Technology  
ksbansal@ucsd.edu

**Dinesh Bharadia**

University of California San Diego  
dbharadia@ucsd.edu

## ABSTRACT

Radar sensors provide reliable perception across adverse weather, lighting, and long-range conditions. Recent advances in foundation models have transformed visual and language understanding, yet their integration with radar sensing remains largely underexplored. Existing radar approaches are fragmented and task-specific; each downstream task employs distinct architectures and training objectives, preventing transfer across tasks. In this work, we introduce RadarFM: a radar foundation model that learns unified scene-level representations through structured spatial language supervision. We make two key contributions: (1) a structured caption framework that encodes vehicle distributions in native radar coordinates, and (2) a hash-aware contrastive learning objective that quantifies continuous scene similarity rather than binary matching, enabling fine-grained spatial reasoning. Leveraging the CARLA simulator, we generate large-scale, well-annotated radar datasets across diverse driving scenarios. We also propose localization-aware metrics that assess spatial accuracy beyond traditional detection measures.

**Keywords** Foundation Models · VLMs · Contrastive Learning · Multimodal Learning · Image Text Alignment · CLIP

## 1 Introduction

Autonomous driving systems require robust perception capabilities that operate reliably across diverse environmental conditions. While cameras and LiDAR have driven recent advances, their performance degrades significantly in adverse weather conditions like rain, fog, and darkness. Radar sensors provide robust, all-weather perception through these adverse weather and lighting conditions [1, 2, 3]. Their ability to directly measure range and velocity makes them indispensable complements to vision-based sensing in autonomous driving. Yet despite these advantages, current machine learning approaches [4, 5, 6, 7, 8] remain fragmented and task-specific. Each downstream task, like object detection, semantic segmentation, and occupancy prediction, employs distinct input encodings, architectural designs, and training objectives [9, 10]. This fragmentation results in learned representations that are non-transferable across tasks and fail to generalize to diverse driving scenarios.

The root of this limitation lies in how radar perception has traditionally been framed. Conventional Radar-ML pipelines [11, 12, 13, 14] focus on narrow, isolated objectives with categorical supervision (e.g., bounding boxes for detection or class labels for segmentation). Such supervision lacks the semantic richness needed to capture the complex spatial relationships and contextual cues critical for autonomous driving, such as which lane a vehicle occupies, whether a pedestrian is crossing, or how traffic infrastructure relates to the ego vehicle’s trajectory.

Recent advances in vision-language models [15, 16, 17] have demonstrated that language grounding offers a scalable and semantically rich supervision signal. Unlike categorical labels, natural language inherently encodes object types, spatial relations, and contextual information (e.g., “a stopped bus 20 m ahead”). Foundation models such as CLIP [18] and BLIP [19] have shown that aligning visual representations with textual descriptions enables transferable features that generalize across diverse tasks and unseen categories. Thus, language acts as a *universal label space*, providing high-level semantics that unify multiple perception objectives under a single representational framework [20, 21].

Translating this paradigm to radar presents both opportunities and challenges. On one hand, language supervision can guide radar encoders to emphasize semantically meaningful objects and their spatial relationships rather than raw signal

patterns. By aligning radar embeddings with descriptive text, we impose semantic structure on radar features. Early explorations [6, 22] have provided preliminary evidence that radar-language alignment can improve downstream scene understanding. On the other hand, existing contrastive learning frameworks rely on binary matching between paired modalities, treating each element in the batch as either perfectly aligned or completely mismatched. This formulation is fundamentally flawed for radar scene understanding, where spatial configurations exist on a continuous spectrum of similarity. This prevents models from learning fine-grained spatial semantics. Training foundation models also requires large-scale, well-annotated datasets with rich textual descriptions, but real-world data collection at scale is quite expensive and time-consuming, posing a significant barrier.

We introduce **RadarFM**, a radar foundation model that integrates language grounding to achieve semantically rich radar scene understanding. To address the data challenge, we leverage the CARLA simulator integrated with a realistic radar sensor [23, 24], enabling large-scale generation of diverse, well-annotated radar data across varied autonomous driving scenarios.

Our approach makes two key contributions. First, we develop a *structured spatial caption framework* that encodes vehicle distributions directly in natural language. Unlike generic descriptions, our captions explicitly ground semantic information in native-sensor spatial coordinates, providing the rich supervision for foundation models to learn meaningful spatial representations. Second, we introduce a *hash-aware contrastive learning* objective that replaces CLIP’s binary matching with continuous scene similarity measures. By quantifying spatial configuration overlap, our loss function enables fine-grained spatial learning rather than coarse keyword matching. Further, we propose localization-aware evaluation metrics that directly assess spatial reasoning beyond traditional detection metrics.

## 2 Related Works

**Existing Radar Perception Approaches** fall into three categories. Task-specific supervised methods train specialized architectures from scratch for individual perception tasks like object detection, segmentation, or scene flow [14, 8, 7, 25, 11, 10, 9]. Cross-modal supervised methods exploit camera and LiDAR supervision to generate pseudo-labels for radar training [4, 13, 11]. Multi-sensor fusion architectures combine radar with cameras or LiDAR to leverage complementary sensor strengths [10, 5]. Unlike these fragmented approaches, we propose learning unified radar representations through structured language supervision that captures semantic richness without relying on task-specific architectures or cross-modal dependencies.

**Vision-Language Foundation Models** have demonstrated the power of natural language acting as a supervision signal for learning transferable visual representations. Contrastive pretraining methods align image and text embeddings in a shared space: CLIP [18] achieves zero-shot transfer across 30+ vision tasks, while [26, 27, 28] scale to billions of noisy image-text pairs to learn robust cross-modal representations. Recent works [29, 30, 16, 15] extend these models to dense prediction tasks through language-aware pretraining, and enable class-free semantic segmentation. These advances collectively demonstrate that language acts as a universal supervision signal [20, 21, 17], enabling models to learn spatially-grounded semantic representations that generalize across tasks without task-specific annotations. Inspired by this paradigm, we propose to leverage language supervision for learning unified radar scene representations.

**CLIP Loss Variants:** The original CLIP [18] framework employs a contrastive loss that treats image-text matching as a binary classification problem. While effective for generic image-level understanding, this binary formulation has inspired numerous extensions [31, 32, 33] like relaxing the one-to-one constraint via soft targets, leveraging label information to pull same-class clusters together while pushing different classes apart, and cluster-level operations through learned prototypes. Some other variants [34, 35, 36] replace softmax normalization with pairwise sigmoid loss, or combine self-supervised and language supervision in a multi-task framework. However, these variants focus on general-purpose vision tasks and fail to address the continuous spectrum of spatial similarity inherent to our problem setup. Our solution addresses this gap by quantifying scene similarity based on spatial configuration overlap, thus enabling fine-grained learning.

## 3 Dataset Curation

Training foundation models requires large-scale datasets with rich and accurate annotations. We leverage the CARLA simulator [37], a well-established platform for autonomous driving research, which provides perfect access to ground truth data for all actors in the scene. This simulator-based approach enables us to collect radar data with precise spatial annotations at scale. Since CARLA’s native radar sensor is highly simplified, we use an open-source implementation [23, 24] which models the propagation behavior of 77 GHz automotive radar very accurately.

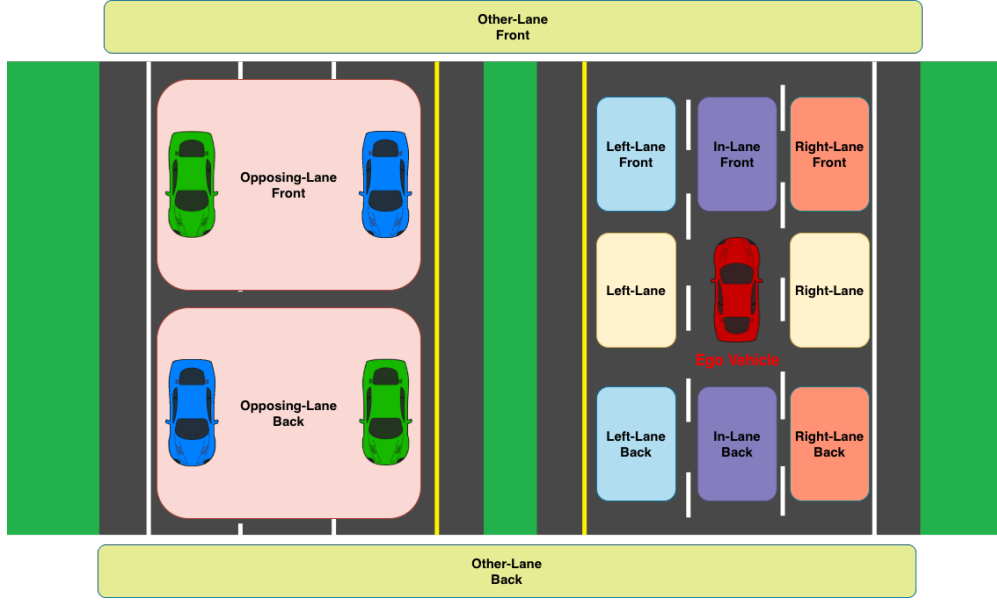


Figure 1: Lane distribution visualization showing the twelve lane-relative angular sectors used for spatial encoding of vehicles relative to the ego vehicle.

**Natural language captions:** The key challenge in creating effective radar-text pairs lies in designing captions that encode spatially-grounded semantics: descriptions that specify *where* objects are located relative to the ego vehicle rather than merely stating their presence. To address this, we develop a structured spatial encoding framework that partitions the radar scene into distance bins and angular sectors, which enables semantically rich descriptions aligned with the radar’s native coordinate system.

We discretize the range of 0-40m into four equal bins. Within each distance bin, we categorize vehicles into 12 lane-relative angular sectors based on their positions and heading vectors relative to the ego vehicle (see Figure 1). This ego-centric spatial encoding provides the foundation for generating structured scene descriptions. The vehicle distribution data of every scene is stored in JSON format. Refer to the supplementary materials for more details.

From the collected JSON representations, we generate natural language captions. Rather than relying on template-based generation, we use LLMs to produce varied descriptions to add diversity among captions. During training, we randomly sample one of the captions for each radar frame, ensuring the model learns from diverse expressions of the same underlying spatial structure. An example scene from the dataset can be seen in Figure 2a with the extracted data in Figure 2b. Here are the captions for the same scene in both structured JSON and natural language formats:

**Structured JSON representation:**

```
{
  "0-10m": {
    "total_vehicles": 3,
    "in_lane_front_side": 1,
    "right_lane_back_side": 2,
  },
  "10-20m": {
    "total_vehicles": 5,
    "in_lane_back_side": 1,
    "right_lane_front_side": 3,
    "right_lane_back_side": 1,
  },
  "20-30m": {
    "total_vehicles": 4,
    "opposing_lane_front": 4,
  },
  "30-40m": {
    "total_vehicles": 2,
  }
}
```

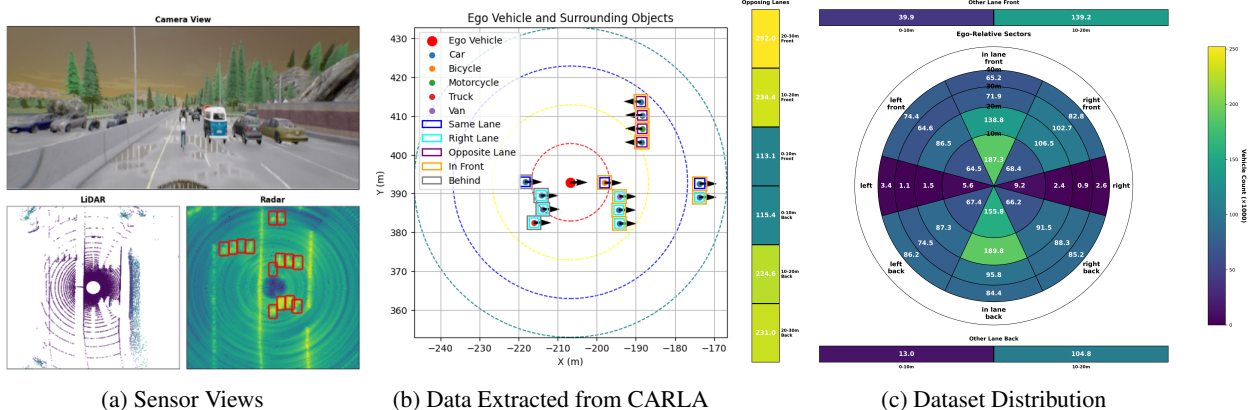


Figure 2: Dataset collection overview. (a) Different sensor viewpoints of a traffic example. (b) Extracted data of vehicles in the scene, with their lane classification. The dashed circles represent distance radii of 10m, 20m, 30m, and 40m. (c) Lane-wise distribution of collected data across the entire dataset represented in radial format.

```

    "in_lane_front_side": 1,
    "right_lane_front_side": 1,
  },
  "applicable_traffic_signs": [],
  "walkers": 0
}

```

**Generated natural language caption:** “ As we are driving, I notice that within the very close range of zero to ten meters from our vehicle, there are three vehicles in total, with one vehicle directly ahead of us in the same lane and two vehicles in the right adjacent lane behind us. Looking a bit further ahead, from ten to twenty meters, I see a total of five vehicles, with three vehicles in the right adjacent lane ahead of us, one vehicle in the right adjacent lane behind us, and one vehicle directly behind us in the same lane. At a moderate distance of twenty to thirty meters, I observe four vehicles in total, all of which are in the opposing lane ahead of us. Further away, from thirty to forty meters, there are two vehicles in total, with one vehicle in the right adjacent lane ahead of us and one vehicle directly ahead of us in the same lane. I also notice that there are no applicable traffic signs around us, and fortunately, there are no walkers on the road. ”

**Hashing of scenes:** To enable efficient scene-similarity computation during contrastive learning, we encode structured spatial information into compact hash vectors. Each scene is represented as a binary hash  $\mathbf{h} \in \{0, 1\}^B$ , where  $B$  is the total number of bits used. The hash structure allocates 4 bits for traffic sign states (traffic light, stop sign, yield sign, and speed limit), 3 bits for pedestrian counts (0-7), and the remaining bits encode vehicle presence in each distance-sector cell. For adjacent lane sectors (left, in-lane, right), we allocate 3 bits per sector, while for opposing and perpendicular lanes, we allocate 5 bits.

**Data collection and statistics:** We collect diverse driving scenarios across CARLA’s urban, highway, and intersection environments under varying traffic densities. For each radar frame, we extract the complete ground truth state of all actors and filter based on the ego vehicle’s location, retaining only objects within the radar’s sensing range. More details can be found in the supplementary material.

We collect over 800,000 radar-caption pairs spanning diverse scenarios: urban intersections with multi-directional traffic flow, highway driving with high-speed vehicles, residential areas with pedestrians, and commonly found intersections. Traffic scenarios range from sparse (1-2 vehicles visible) to dense (10+ vehicles), ensuring the model learns across varying complexity levels. The distribution of the number of vehicles across the entire dataset can be seen in Figure 2c. This dataset is, to our knowledge, the first large-scale radar dataset with structured, spatially-grounded natural language descriptions, and we will release it to facilitate future research.

## 4 RadarFM: Architecture and Approach

Our framework, RadarFM, consists of two key components: a CLIP-based [18, 38] Vision encoder for radar heatmaps and a GPT-2-like Transformer [39, 40] encoder for captions, (2) hash-aware contrastive learning that accounts for continuous scene similarity. Additionally, we introduce a generative captioning capability that serves as a diagnostic tool to validate the learned representations.

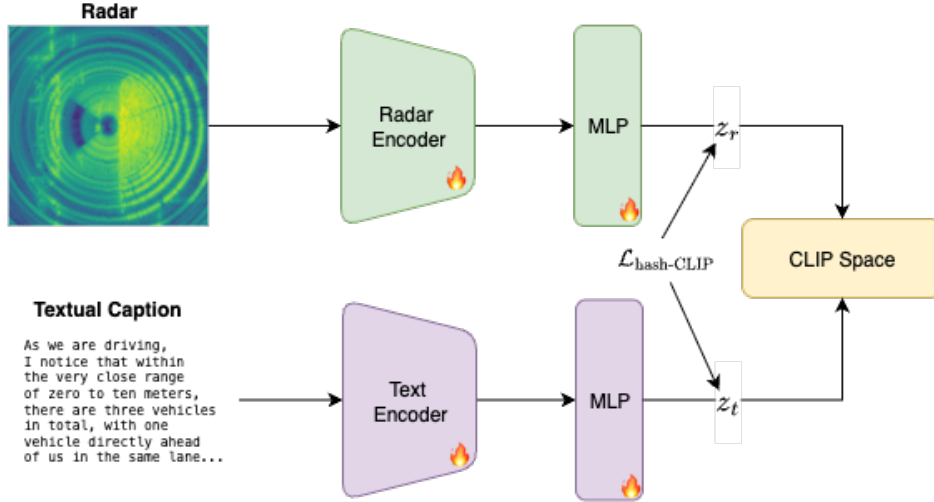


Figure 3: **The Pre-training phase.** Radar range-angle heatmaps are encoded via ViT-B/16 backbone, while captions are processed through a GPT-2-like transformer encoder. The radar and text embeddings are projected into a shared 512-dimensional space where hash-aware contrastive learning aligns semantically similar scenes based on spatial configuration overlap.

#### 4.1 Pre-training Architecture

We adopt the pretrained ViT-B/16 encoder from CLIP [18], leveraging its robust visual feature extraction capabilities developed on large-scale image-text data. Given a radar range-angle heatmap, we replicate it across three channels to match CLIP’s expected input format. The heatmap is partitioned into  $16 \times 16$  patches with learnable positional embeddings, and the classification token output  $\mathbf{z}_r \in \mathbb{R}^{512}$  serves as our radar scene representation (Figure 3).

For text encoding, our captions frequently exceed CLIP’s maximum token limit of 77 tokens due to their detailed enumeration, and so we extended the context window to 400 tokens and trained the encoder from scratch. Both embeddings are then projected into a shared 512-dimensional space with MLPs.

#### 4.2 Hash-Aware Contrastive Learning

Standard contrastive learning frameworks like CLIP [18] treat sample pairs as binary: a matched image-text pair is positive (label = 1), while all other pairs in the batch are negative (label = 0). This binary formulation is suboptimal for radar scene understanding because scene similarity lies on a continuous spectrum (see the supplementary material for examples). Having binary labels will harshly penalize the model from learning fine-grained spatial distinctions, and instead drives it toward coarse, keyword-based matching.

To address this, we propose a hash-aware contrastive learning objective that quantifies scene similarity based on spatial configuration overlap. Recall from Section 3 that each scene is encoded as a binary hash vector  $\mathbf{h} \in \{0, 1\}^B$ , where  $B$  is the total number of bits and it encodes vehicle count in a specific distance-sector cell. We use this representation to compute soft similarity targets between scenes.

**Hamming distance as scene dissimilarity:** For two scenes  $i$  and  $j$  with hash vectors  $\mathbf{h}_i$  and  $\mathbf{h}_j$ , we compute the Hamming distance for each distance bin  $b$  as:

$$d_H(\mathbf{h}_i^{(b)}, \mathbf{h}_j^{(b)}) = \text{popcount}(\mathbf{h}_i^{(b)} \oplus \mathbf{h}_j^{(b)}) \quad (1)$$

where  $\mathbf{h}_i^{(b)}$  denotes the sub-vector of  $\mathbf{h}_i$  corresponding to distance bin  $b$ ,  $\oplus$  is the bitwise XOR operation, and popcount counts the number of differing bits. Intuitively,  $d_H$  measures how many spatial cells differ in vehicle occupancy between the two scenes.

**Gaussian kernel for soft similarity:** We convert Hamming distances into soft similarity scores using a Gaussian kernel:

$$s_{ij}^{(b)} = \exp\left(-\frac{d_H^2(\mathbf{h}_i^{(b)}, \mathbf{h}_j^{(b)})}{2\sigma_b^2}\right) \quad (2)$$

where  $\sigma_b$  is a distance-dependent bandwidth parameter. The key insight is that not all spatial errors are equally critical in autonomous driving: mislocalization in the near field (0-10m) poses immediate safety risks, whereas far-field errors (30-40m) are more tolerable as they affect strategic planning rather than immediate control. To encode this priority, we use reducing values of  $\sigma_b$  as the distance increases, which yields tighter matching (smaller  $\sigma$ ) for close bins and looser matching (larger  $\sigma$ ) for far bins.

**Distance-dependent weighting:** Beyond adaptive bandwidths, we explicitly prioritize near-field accuracy by applying exponentially decaying weights across distance bins:

$$w_b = \lambda^{b-1}, \quad \lambda \in (0, 1] \quad (3)$$

where  $\lambda$  controls the decay rate (we use  $\lambda = 0.85$ ). This ensures that errors in the 0-10m bin contribute more strongly to the loss than errors in the 30-40m bin.

**Soft target matrix:** Combining the per-bin similarities with distance weights, we construct a soft target matrix  $\mathbf{T}^{\text{soft}}$  for each batch:

$$T_{ij}^{\text{soft}} = \frac{\sum_{b=1}^{B_{\text{dist}}} w_b \cdot s_{ij}^{(b)}}{\sum_{k=1}^N \sum_{b=1}^{B_{\text{dist}}} w_b \cdot s_{ik}^{(b)}} \quad (4)$$

where  $N$  is the batch size. Normalization across all samples  $k$  ensures that  $\sum_j T_{ij}^{\text{soft}} = 1$ , maintaining a valid probability distribution.

**Modified CLIP loss:** Given radar embeddings  $\mathbf{z}_r^i$  and text embeddings  $\mathbf{z}_t^j$  for a batch of  $N$  samples, we compute pairwise cosine similarities:

$$S_{ij} = \frac{\mathbf{z}_r^i \cdot \mathbf{z}_t^j}{\|\mathbf{z}_r^i\| \|\mathbf{z}_t^j\|} \quad (5)$$

The hash-aware CLIP loss replaces the standard hard cross-entropy with a soft variant:

$$\mathcal{L}_{r \rightarrow t} = -\frac{1}{N} \sum_{i=1}^N \sum_{j=1}^N T_{ij}^{\text{soft}} \log \frac{\exp(S_{ij}/\tau)}{\sum_{k=1}^N \exp(S_{ik}/\tau)} \quad (6)$$

where  $\tau$  is a temperature hyperparameter (we use  $\tau = 0.07$ , following CLIP). The symmetric text-to-radar loss  $\mathcal{L}_{t \rightarrow r}$  is defined analogously. The final contrastive loss is:

$$\mathcal{L}_{\text{hash-CLIP}} = \frac{1}{2} (\mathcal{L}_{r \rightarrow t} + \mathcal{L}_{t \rightarrow r}) \quad (7)$$

This formulation provides two key advantages over standard CLIP:

- **Fine-grained spatial learning:** The model avoids harsh penalties for placing similar scenes close together in embedding space. Scenes differing by one vehicle receive partial credit rather than being treated as completely dissimilar, enabling learning of precise spatial distinctions.
- **Scalable supervision:** Soft labels are computed automatically from spatial structure without requiring human annotation, allowing to scale naturally to large datasets.

**Batch size considerations:** The effectiveness of soft contrastive learning depends critically on batch diversity. With hard labels, a small batch suffices, but with soft labels, however, the model must learn from gradient signals arising from many partially-similar examples with varying degrees of overlap. Empirically, we find that batch sizes upwards of 120 are necessary to provide sufficient diversity for training.

### 4.3 Generative Captioning for Validation

Does contrastive pretraining truly learn spatially-grounded semantic understanding? To validate that RadarFM captures genuine scene comprehension, we extend our framework with generative captioning capabilities (Figure 4). Taking inspiration from ClipCap [41], we train a lightweight projection mechanism from our pretrained radar encoder to GPT-2’s [39] embedding space. This generative task serves as a *diagnostic tool* that assesses whether the model can produce accurate, detailed captions from radar inputs alone.

**Frozen Text Encoder:** We freeze the weights of our pretrained text encoder to preserve the rich multimodal representations. It produces a fixed-dimensional embedding  $\mathbf{z}_t \in \mathbb{R}^{512}$  for each input text caption. Crucially, we want to align the

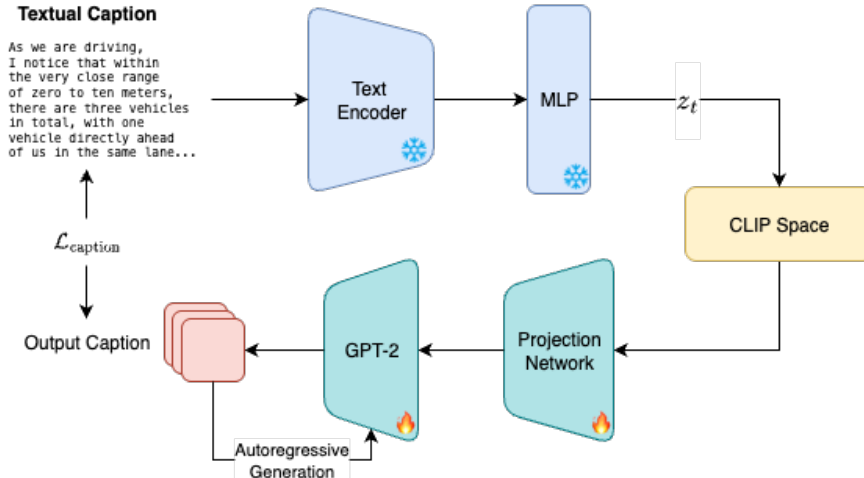


Figure 4: **Fine-tuning phase with generative captioning.** The pre-trained text encoder is frozen, and a lightweight transformer-based mapping network projects radar embeddings into GPT-2’s input space. This enables post-training autoregressive generation with radar embeddings as input to the projection network.

text encoder’s embeddings with the output caption rather than the radar’s embeddings, as during deployment, only the radar modality will be present.

**Lightweight Mapping Network:** The transformer-based mapping network  $f_\theta$  projects the text embeddings into the input space of GPT-2 [39]. This network generates expressive prefix embeddings through cross-attention mechanisms [41], which is critical when the language model remains frozen, as the mapping network must encode all spatial information into a fixed-length prefix that can effectively steer GPT-2’s generation process. These prefix embeddings act as a soft prompt that conditions the auto-regressive generation. This design also substantially reduces the trainable parameters.

During training, we optimize the mapping network  $f_\theta$  to minimize the cross-entropy loss over generated caption tokens:

$$\mathcal{L}_{caption} = - \sum_{t=1}^T \log p_{\text{GPT}}(c_t | \mathbf{p}_{1:k}, c_{1:t-1}) \quad (8)$$

where  $c_t$  is the  $t$ -th token in the ground-truth caption, and  $T$  is the caption length. This follows from the typical teacher-forcing [42] training methodology.

**Inference-time caption generation:** During inference time, we project the radar heatmap onto the CLIP space using the trained vision encoder and then pass these embeddings to the Transformer-based projection network for caption generation.

## 5 Experiments

**Training Setup:** The pre-training phase used a batch size of 160, whereas the caption generation training used a batch size of 60, and both ran for 50 epochs until the validation accuracy plateaued. Both methods used the AdamW optimizer with standard parameters and a learning rate of  $1 \times 10^{-5}$ . Training was conducted on a server equipped with 4 NVIDIA A100 GPUs; the pre-training process completed in 12.5 hours, and caption generation training required 25 hours. Both training phases used a standard 80-20 train-test split of our collected dataset.

We evaluate RadarFM through two complementary perspectives: (1) analyzing the quality of learned radar representations from hash-aware contrastive pre-training, and (2) assessing spatial understanding through generative captioning performance.

### 5.1 Pre-training Quality: Attention Analysis

To validate that hash-aware contrastive learning produces spatially-grounded representations, we analyze the attention patterns learned by the frozen ViT encoder. We employ attention rollout [43], which recursively multiplies attention weights across transformer layers to reveal cumulative attention flow from the classification token to input patches.

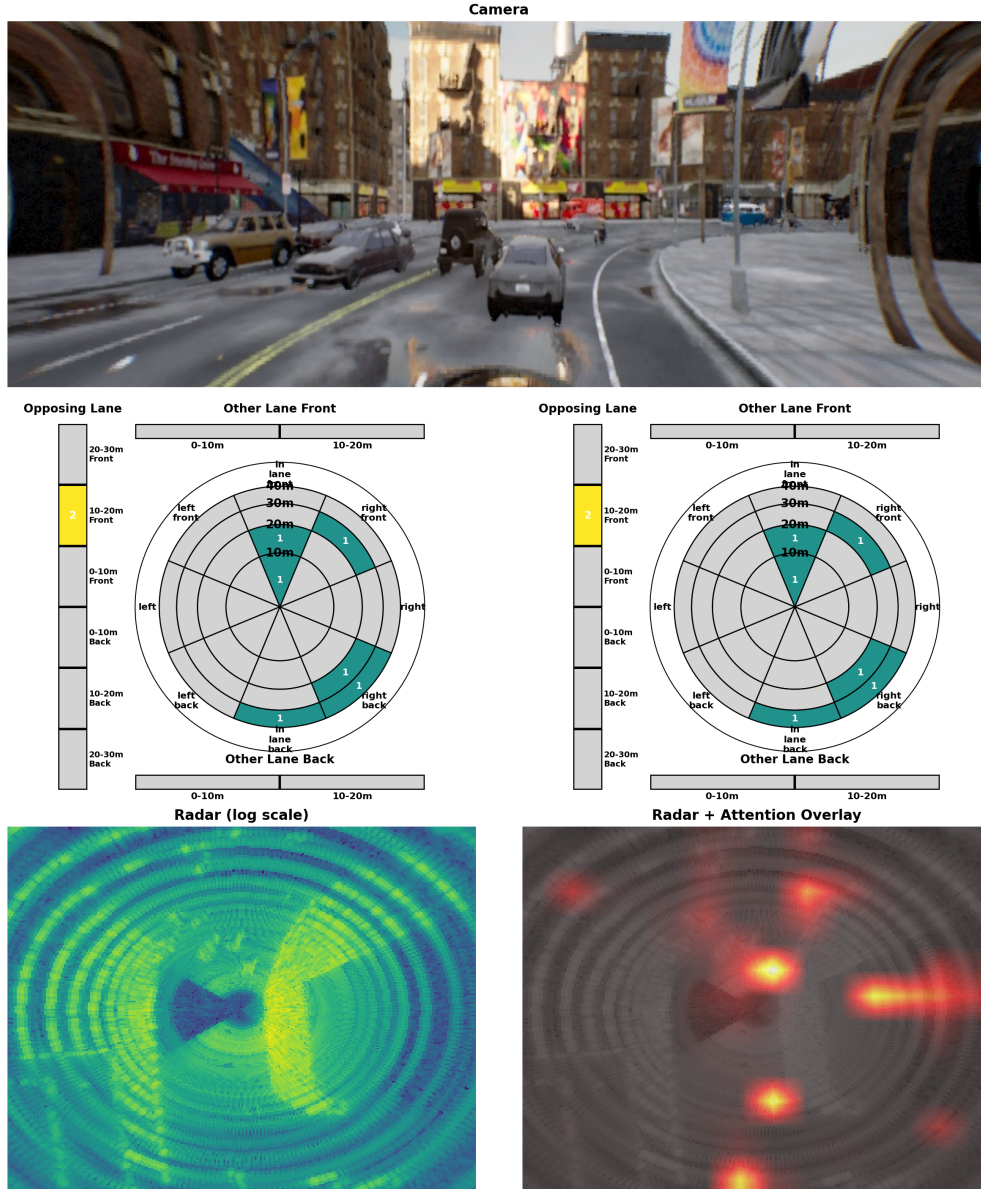


Figure 5: **Attention rollout visualization from pre-trained radar encoder.** Top: Camera reference image. Middle: Ground truth (left) and predicted (right) vehicle distributions in radial format across distance bins and angular sectors. Bottom: Radar range-angle heatmap (left) and attention rollout overlay (right) showing cumulative attention weights from the final three transformer layers. The attention weights concentrate precisely on regions containing vehicles, validating the effectiveness of hash-aware contrastive learning.

Figure 5 visualizes attention rollout for a representative scene from our test set. We aggregate attention weights from the final three transformer layers (layers 10-12) of the ViT-B/16 encoder, overlay them on the radar heatmap, and compare against ground truth vehicle positions. The visualization reveals that attention concentrates precisely on spatial regions containing vehicles, with minimal or no weight allocated to empty sectors. This alignment provides direct evidence that our hash-aware contrastive objective successfully teaches the encoder to emphasize semantically relevant spatial structures.

We include additional attention rollout videos showing continuous ego vehicle trajectories with frame-by-frame caption predictions in the supplementary materials.

## 5.2 Localization-Aware Evaluation

The above attention analysis validates the quality of pre-trained representations, but the ultimate test of spatial understanding is whether the model can generate accurate scene descriptions. We evaluate this through generative captioning with localization-aware metrics.

## 5.3 Metrics

While standard captioning metrics such as BLEU [44], METEOR [45], and CIDEr [46] effectively measure n-gram overlap, they are fundamentally flawed to assess the spatial accuracy. These metrics treat captions as bags of words or phrases, rewarding lexical similarity without verifying whether the spatial information is correct. To address this critical gap, we propose novel localization-aware metrics that directly quantify spatial reasoning accuracy by measuring how precisely the model predicts vehicle positions in the radar’s native coordinate system.

We adapt the standard precision, recall, and F-score metrics for evaluating the spatial accuracy of predicted vehicle positions, structured by distance bins and angular sectors.

### 5.3.1 Adapted Precision and Recall

Our evaluation operates at the granularity of distance-sector cells, matching the structured representation used in our hash encoding (Section 3). For each distance-sector cell  $(b, s)$ , let  $y$  denote the ground-truth vehicle count and  $\hat{y}$  denote the predicted count extracted from the generated caption. We define the fundamental counting metrics as:

$$\text{TP} = \min(\hat{y}, y) \tag{9}$$

$$\text{FP} = \max(0, \hat{y} - y) \tag{10}$$

$$\text{FN} = \max(0, y - \hat{y}) \tag{11}$$

Note that we do not consider true negatives (TN) in our formulation, as our structured captions do not explicitly predict the absence of vehicles in a given sector; they only enumerate vehicles that are present. Based on these counting metrics, precision and recall for each cell are defined as:

$$\text{Precision}_{bs} = \begin{cases} 1 & \text{if } \hat{y} = y \text{ (perfect match)} \\ \frac{y}{\hat{y}} & \text{if } \hat{y} > y \text{ (over-counting)} \\ 1 & \text{if } \hat{y} < y \text{ (under-counting)} \end{cases} \tag{12}$$

$$\text{Recall}_{bs} = \begin{cases} 1 & \text{if } \hat{y} = y \text{ (perfect match)} \\ 1 & \text{if } \hat{y} > y \text{ (over-counting)} \\ \frac{\hat{y}}{y} & \text{if } \hat{y} < y \text{ (under-counting)} \end{cases} \tag{13}$$

### 5.3.2 Dataset-Level Aggregation via Micro-Averaging

To compute dataset-level metrics, we employ micro-averaging, which aggregates true positives, false positives, and false negatives across all test scenes before computing precision and recall. This approach weights each vehicle equally, regardless of scene complexity. For each distance-sector cell  $(b, s)$ , we sum the counts across all  $N$  test scenes:

$$\text{TP}_{bs} = \sum_{i=1}^N \min(\hat{y}_{bs}^{(i)}, y_{bs}^{(i)}) \tag{14}$$

$$\text{FP}_{bs} = \sum_{i=1}^N \max(0, \hat{y}_{bs}^{(i)} - y_{bs}^{(i)}) \tag{15}$$

$$\text{FN}_{bs} = \sum_{i=1}^N \max(0, y_{bs}^{(i)} - \hat{y}_{bs}^{(i)}) \tag{16}$$

The dataset-level precision, recall, and F1 score for each cell  $(b, s)$  are then computed independently using standard formulas.

### 5.3.3 Advantages Over Standard Metrics

Our localization-aware metrics provide three key advantages:

- **Spatial grounding:** This metric directly assesses whether the model understands where objects are located.
- **Interpretability:** Precision and recall have clear semantic meaning in the context of vehicle detection, making results easy to interpret.
- **Fine-grained analysis:** Cell-wise evaluation enables detailed diagnosis of failure modes (e.g., does the model struggle with left vs. right? Near vs. far?).

## 5.4 Generative Captioning Performance

In this evaluation, the model generates natural language scene descriptions, which are parsed using an LLM to extract structured JSON representations containing vehicle counts per distance-sector cell. These predictions are compared against ground truth using our localization-aware metrics (Section 5.3).

### 5.4.1 Unified vs. Distance-Stratified Models

Training a unified model to handle all distance ranges simultaneously revealed suboptimal performance in far-field regions (20-40m), with F1 scores dropping to 0.28 and 0.21 for the 20-30m and 30-40m bins, respectively (Table 1). Investigating this limitation, we observed a significant data imbalance in our training set: Figure 2c shows that samples contain substantially more vehicles in close-range sectors (0-20m) compared to far-range sectors (20-40m).

To address this performance gap, we train two specialized models: one for close-range (0-20m) and another for far-range (20-40m). Each model trains exclusively on its distance range. Table 1 quantifies the improvement achieved by this distance-stratified approach, which consistently outperforms the unified model across all distance bins, with particularly dramatic improvements in far-field regions: F1 scores increase by 0.32 (114.8%) in the 20-30m bin and 0.21 (101%) in the 30-40m bin.

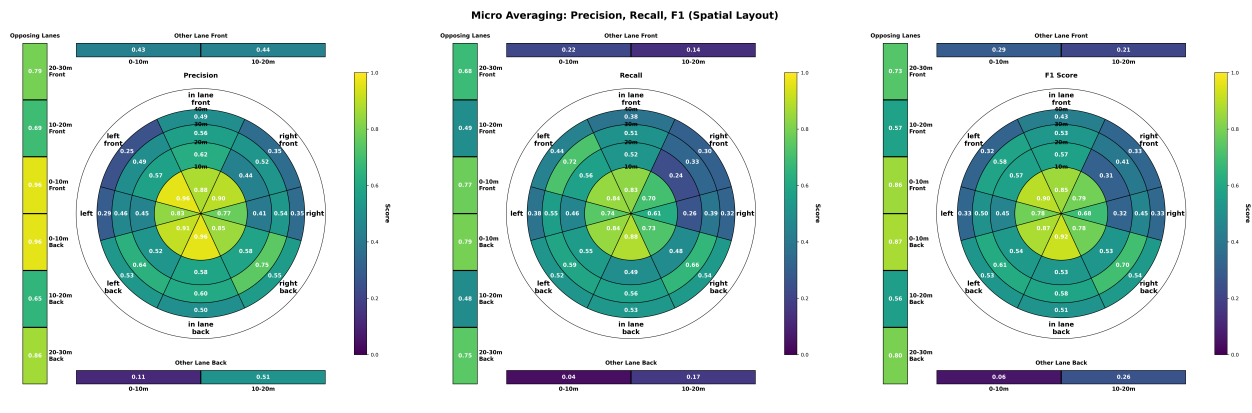


Figure 6: **Distance-stratified model localization performance.** Precision, recall, and F1 scores across all distance bins and angular sectors. Each subplot shows results for the twelve angular sectors within a distance bin. The specialized far-range model achieves F1 scores above 0.5 in the 20-30m bin, substantially outperforming the unified model (see Table 1). Near-field bins (0-10m, 10-20m) maintain high performance across most sectors.

### 5.4.2 Spatial Performance Analysis

Figure 6 provides a fine-grained view of the distance-stratified model’s performance across all distance-sector cells. The heatmaps reveal several key patterns. First, near-field bins (0-10m, 10-20m) consistently achieve high F1 scores across most angular sectors, validating that our model learns accurate close-range spatial understanding. Second, the specialized far-range model successfully mitigates the data imbalance problem, achieving F1 scores above 0.5 in the 20-30m bin and above 0.3 in the 30-40m bin.

Third, performance varies across angular sectors in interpretable ways. The opposing lanes (front and back) achieve the highest F1 scores because highway driving scenarios, which dominate our dataset, feature prominent opposing traffic. In-lane sectors (front and back) also perform well, as the ego vehicle naturally observes more traffic in its own lane.

Table 1: **Unified vs. distance-stratified model comparison.** F1 scores (arithmetic mean) averaged across all angular sectors for each distance bin. The distance-stratified approach yields substantial improvements, particularly in far-field regions where training data is scarce.

Model	0–10m	10–20m	20–30m	30–40m
Unified	0.696	<b>0.471</b>	0.275	0.206
Distance-Stratified	<b>0.781</b>	0.450	<b>0.590</b>	<b>0.414</b>
Improvement	+0.085	-0.021	+0.315	+0.208
Relative Gain	+12.2%	-4.5%	+114.5%	+100.9%

Table 2: **F1 scores by angular sector.** Performance (arithmetic mean) averaged across all distance bins for each angular sector. The distance-stratified model consistently outperforms the unified model across most sectors.

Model	Opp. Lane Back	Opp. Lane Front	Right Lane Back	In Lane Back	Left Lane Back	In Lane Front	Left Lane Front	Left Side	Right Lane Front	Right Side	Other Lane Back	Other Lane Front
Unified	0.530	0.540	0.437	0.516	0.465	0.482	0.502	0.384	0.409	0.324	0.203	<b>0.363</b>
Distance-Stratified	<b>0.741</b>	<b>0.721</b>	<b>0.638</b>	<b>0.637</b>	<b>0.637</b>	<b>0.595</b>	<b>0.590</b>	<b>0.517</b>	<b>0.456</b>	<b>0.447</b>	<b>0.256</b>	0.251
Improvement	+0.211	+0.181	+0.201	+0.121	+0.172	+0.113	+0.088	+0.133	+0.047	+0.123	+0.053	-0.112
Relative Gain	+39.8%	+33.5%	+46.0%	+23.4%	+37.0%	+23.4%	+17.5%	+34.6%	+11.5%	+38.0%	+26.1%	-30.9%

Side lanes and perpendicular sectors show more variable performance, consistent with their sparser representation in typical driving scenarios.

During inference, predictions from both specialized models are combined to produce complete scene descriptions spanning the full 0-40m range.

### 5.4.3 Cross-Sector Performance

Table 2 examines performance across different angular sectors, averaged over all distance bins. This view reveals which spatial regions the model handles well versus those that remain challenging. Opposing lanes achieve the highest F1 scores (0.741 back, 0.721 front), followed by in-lane and adjacent lane sectors (0.590 front, 0.638 back). Side sectors and perpendicular lanes show lower performance (0.251, 0.517 side), reflecting both their geometric complexity and their relative scarcity in the training distribution.

## 6 Conclusions

We present RadarFM, a radar foundation model that learns spatially-grounded scene representations through structured language supervision. By introducing structured captions that encode vehicle distributions in native radar coordinates and a hash-aware contrastive learning objective that quantifies continuous scene similarity, RadarFM learns fine-grained spatial understanding rather than coarse keyword matching. We contribute a large-scale dataset of over 800,000 radar-caption pairs and novel localization-aware evaluation metrics that directly assess spatial reasoning accuracy beyond traditional linguistic similarity measures.

Future work will focus on demonstrating that RadarFM’s learned representations provide sufficient information for end-to-end driving tasks and sim-to-real transfer to work with real-world radar datasets.

## References

- [1] Fatemeh Norouzian, Emidio Marchetti, Edward Hoare, Marina Gashinova, Costas Constantinou, Peter Gardner, and Mikhail Cherniakov. Experimental study on low-thz automotive radar signal attenuation during snowfall. *IET Radar, Sonar & Navigation*, 13(9):1421–1427, 2019.
- [2] Fatemeh Norouzian, Emidio Marchetti, Marina Gashinova, Edward Hoare, Costas Constantinou, Peter Gardner, and Mikhail Cherniakov. Rain attenuation at millimeter wave and low-thz frequencies. *IEEE Transactions on Antennas and Propagation*, 68(1):421–431, 2019.
- [3] Shizhe Zang, Ming Ding, David Smith, Paul Tyler, Thierry Rakotoarivelo, and Mohamed Ali Kaafar. The impact of adverse weather conditions on autonomous vehicles: How rain, snow, fog, and hail affect the performance of a self-driving car. *IEEE vehicular technology magazine*, 14(2):103–111, 2019.
- [4] Kshitiz Bansal, Keshav Rungta, and Dinesh Bharadia. Radsegnet: A reliable approach to radar camera fusion, 2022.

- [5] Kshitiz Bansal, Keshav Rungta, Siyuan Zhu, and Dinesh Bharadia. Pointillism: Accurate 3d bounding box estimation with multi-radars. In *Proceedings of the 18th Conference on Embedded Networked Sensor Systems*, pages 340–353, 2020.
- [6] Yiduo Hao, Sohrab Madani, Junfeng Guan, Mohammed Alloulah, Saurabh Gupta, and Haitham Hassanieh. Bootstrapping autonomous driving radars with self-supervised learning. In *Proceedings - 2024 IEEE/CVF Conference on Computer Vision and Pattern Recognition, CVPR 2024*, Proceedings of the IEEE Computer Society Conference on Computer Vision and Pattern Recognition, pages 15012–15023. IEEE Computer Society, 2024. Publisher Copyright: © 2024 IEEE.; 2024 IEEE/CVF Conference on Computer Vision and Pattern Recognition, CVPR 2024 ; Conference date: 16-06-2024 Through 22-06-2024.
- [7] Ao Zhang, Farzan Erlik Nowruzi, and Robert Laganriere. Raddet: Range-azimuth-doppler based radar object detection for dynamic road users. In *2021 18th Conference on Robots and Vision (CRV)*, pages 95–102. IEEE, 2021.
- [8] Sohrab Madani, Jayden Guan, Waleed Ahmed, Saurabh Gupta, and Haitham Hassanieh. Radatron: Accurate detection using multi-resolution cascaded mimo radar. In *European Conference on Computer Vision*, pages 160–178. Springer, 2022.
- [9] Tianshu Huang, Akarsh Prabhakara, Chuhan Chen, Jay Karhade, Deva Ramanan, Matthew O’toole, and Anthony Rowe. Towards foundational models for single-chip radar. In *Proceedings of the IEEE/CVF International Conference on Computer Vision*, pages 24655–24665, 2025.
- [10] Xiaomeng Chu, Jiajun Deng, Guoliang You, Yifan Duan, Houqiang Li, and Yanyong Zhang. Racformer: Towards high-quality 3d object detection via query-based radar-camera fusion. In *Proceedings of the Computer Vision and Pattern Recognition Conference*, pages 17081–17091, 2025.
- [11] Fangqiang Ding, Andras Palffy, Darius M Gavrilă, and Chris Xiaoxuan Lu. Hidden gems: 4d radar scene flow learning using cross-modal supervision. In *Proceedings of the IEEE/CVF Conference on Computer Vision and Pattern Recognition*, pages 9340–9349, 2023.
- [12] Prannay Kaul, Daniele De Martini, Matthew Gadd, and Paul Newman. Rss-net: Weakly-supervised multi-class semantic segmentation with fmcw radar. In *2020 IEEE Intelligent Vehicles Symposium (IV)*, pages 431–436. IEEE, 2020.
- [13] Itai Orr, Moshik Cohen, and Zeev Zalevsky. High-resolution radar road segmentation using weakly supervised learning. *Nature Machine Intelligence*, 3(3):239–246, 2021.
- [14] Yizhou Wang, Zhongyu Jiang, Xiangyu Gao, Jenq-Neng Hwang, Guanbin Xing, and Hui Liu. Rodnet: Radar object detection using cross-modal supervision. In *Proceedings of the IEEE/CVF Winter Conference on Applications of Computer Vision*, pages 504–513, 2021.
- [15] Wenbin He, Suphanut Jamonnak, Liang Gou, and Liu Ren. Clip-s4: Language-guided self-supervised semantic segmentation. In *Proceedings of the IEEE/CVF conference on computer vision and pattern recognition*, pages 11207–11216, 2023.
- [16] Zheng Ding, Jieke Wang, and Zhuowen Tu. Open-vocabulary universal image segmentation with maskclip. *arXiv preprint arXiv:2208.08984*, 2022.
- [17] Yongchao Feng, Yajie Liu, Shuai Yang, Wenrui Cai, Jinqing Zhang, Qiqi Zhan, Ziyue Huang, Hongxi Yan, Qiao Wan, Chenguang Liu, Junzhe Wang, Jiahui Lv, Ziqi Liu, Tengyuan Shi, Qingjie Liu, and Yunhong Wang. Vision-language model for object detection and segmentation: A review and evaluation, 2025.
- [18] Alec Radford, Jong Wook Kim, Chris Hallacy, Aditya Ramesh, Gabriel Goh, Sandhini Agarwal, Girish Sastry, Amanda Askell, Pamela Mishkin, Jack Clark, et al. Learning transferable visual models from natural language supervision. In *International conference on machine learning*, pages 8748–8763. PMLR, 2021.
- [19] Junnan Li, Dongxu Li, Silvio Savarese, and Steven Hoi. Blip-2: bootstrapping language-image pre-training with frozen image encoders and large language models. In *Proceedings of the 40th International Conference on Machine Learning, ICML’23*. JMLR.org, 2023.
- [20] Alexander Kirillov, Eric Mintun, Nikhila Ravi, Hanzi Mao, Chloe Rolland, Laura Gustafson, Tete Xiao, Spencer Whitehead, Alexander C. Berg, Wan-Yen Lo, Piotr Dollar, and Ross Girshick. Segment anything. In *Proceedings of the IEEE/CVF International Conference on Computer Vision (ICCV)*, pages 4015–4026, October 2023.
- [21] Nikhila Ravi, Valentin Gabeur, Yuan-Ting Hu, Ronghang Hu, Chaitanya Ryali, Tengyu Ma, Haitham Khedr, Roman Rädle, Chloe Rolland, Laura Gustafson, Eric Mintun, Junting Pan, Kalyan Vasudev Alwala, Nicolas Carion, Chao-Yuan Wu, Ross Girshick, Piotr Dollár, and Christoph Feichtenhofer. Sam 2: Segment anything in images and videos, 2024.

- [22] Mariia Pushkareva, Yuri Feldman, Csaba Domokos, Kilian Rambach, and Dotan Di Castro. Radar spectra-language model for automotive scene parsing, 2024.
- [23] Satyam Srivastava, Jerry Li, Pushkal Mishra, Kshitiz Bansal, and Dinesh Bharadia. A realistic radar simulator for end-to-end autonomous driving in carla. In *2025 IEEE 102nd Vehicular Technology Conference (VTC2025-Fall)*, pages 1–6, 2025.
- [24] Pushkal Mishra, Satyam Srivastava, Jerry Li, Kshitiz Bansal, and Dinesh Bharadia. *Demo Abstract: C-Shenron: A Realistic Radar Simulation Framework for CARLA*, page 726–727. Association for Computing Machinery, New York, NY, USA, 2025.
- [25] Dong-Hee Paek, Seung-Hyun Kong, and Kevin Tirta Wijaya. K-radar: 4d radar object detection for autonomous driving in various weather conditions. *Advances in Neural Information Processing Systems*, 35:3819–3829, 2022.
- [26] Chao Jia, Yinfei Yang, Ye Xia, Yi-Ting Chen, Zarana Parekh, Hieu Pham, Quoc Le, Yun-Hsuan Sung, Zhen Li, and Tom Duerig. Scaling up visual and vision-language representation learning with noisy text supervision. In *International conference on machine learning*, pages 4904–4916. PMLR, 2021.
- [27] Jiahui Yu, Zirui Wang, Vijay Vasudevan, Legg Yeung, Mojtaba Seyedhosseini, and Yonghui Wu. Coca: Contrastive captioners are image-text foundation models. *arXiv preprint arXiv:2205.01917*, 2022.
- [28] Lu Yuan, Dongdong Chen, Yi-Ling Chen, Noel Codella, Xiyang Dai, Jianfeng Gao, Houdong Hu, Xuedong Huang, Boxin Li, Chunyuan Li, et al. Florence: A new foundation model for computer vision. *arXiv preprint arXiv:2111.11432*, 2021.
- [29] Liunian Harold Li, Pengchuan Zhang, Haotian Zhang, Jianwei Yang, Chunyuan Li, Yiwu Zhong, Lijuan Wang, Lu Yuan, Lei Zhang, Jenq-Neng Hwang, Kai-Wei Chang, and Jianfeng Gao. Grounded language-image pre-training. In *Proceedings of the IEEE/CVF Conference on Computer Vision and Pattern Recognition (CVPR)*, pages 10965–10975, June 2022.
- [30] Yiwu Zhong, Jianwei Yang, Pengchuan Zhang, Chunyuan Li, Noel Codella, Liunian Harold Li, Luwei Zhou, Xiyang Dai, Lu Yuan, Yin Li, and Jianfeng Gao. Regionclip: Region-based language-image pretraining. In *Proceedings of the IEEE/CVF Conference on Computer Vision and Pattern Recognition (CVPR)*, pages 16793–16803, June 2022.
- [31] Yuting Gao, Jinfeng Liu, Zihan Xu, Tong Wu, Enwei Zhang, Ke Li, Jie Yang, Wei Liu, and Xing Sun. Softclip: softer cross-modal alignment makes clip stronger. In *Proceedings of the Thirty-Eighth AAAI Conference on Artificial Intelligence and Thirty-Sixth Conference on Innovative Applications of Artificial Intelligence and Fourteenth Symposium on Educational Advances in Artificial Intelligence, AAAI’24/IAAI’24/EAAI’24*. AAAI Press, 2024.
- [32] Prannay Khosla, Piotr Teterwak, Chen Wang, Aaron Sarna, Yonglong Tian, Phillip Isola, Aaron Maschinot, Ce Liu, and Dilip Krishnan. Supervised contrastive learning. In *Proceedings of the 34th International Conference on Neural Information Processing Systems, NIPS ’20*, Red Hook, NY, USA, 2020. Curran Associates Inc.
- [33] Junnan Li, Pan Zhou, Caiming Xiong, and Steven Hoi. Prototypical contrastive learning of unsupervised representations. In *International Conference on Learning Representations*, 2021.
- [34] Xiaohua Zhai, Basil Mustafa, Alexander Kolesnikov, and Lucas Beyer. Sigmoid loss for language image pre-training. In *Proceedings of the IEEE/CVF international conference on computer vision*, pages 11975–11986, 2023.
- [35] Norman Mu, Alexander Kirillov, David Wagner, and Saining Xie. Slip: Self-supervision meets language-image pre-training. In *European conference on computer vision*, pages 529–544. Springer, 2022.
- [36] Zehan Wang, Sashuai Zhou, Shaoxuan He, Haifeng Huang, Lihe Yang, Ziang Zhang, Xize Cheng, Shengpeng Ji, Tao Jin, Hengshuang Zhao, et al. Spatialclip: Learning 3d-aware image representations from spatially discriminative language. In *Proceedings of the Computer Vision and Pattern Recognition Conference*, pages 29656–29666, 2025.
- [37] Alexey Dosovitskiy, German Ros, Felipe Codevilla, Antonio Lopez, and Vladlen Koltun. Carla: An open urban driving simulator, 2017.
- [38] Alexey Dosovitskiy, Lucas Beyer, Alexander Kolesnikov, Dirk Weissenborn, Xiaohua Zhai, Thomas Unterthiner, Mostafa Dehghani, Matthias Minderer, Georg Heigold, Sylvain Gelly, Jakob Uszkoreit, and Neil Houlsby. An image is worth 16x16 words: Transformers for image recognition at scale. In *International Conference on Learning Representations*, 2021.
- [39] Alec Radford, Jeffrey Wu, Rewon Child, David Luan, Dario Amodei, and Ilya Sutskever. Language models are unsupervised multitask learners. *OpenAI*, 2019. Accessed: 2024-11-15.

- [40] Ashish Vaswani, Noam Shazeer, Niki Parmar, Jakob Uszkoreit, Llion Jones, Aidan N Gomez, Łukasz Kaiser, and Illia Polosukhin. Attention is all you need. *Advances in neural information processing systems*, 30, 2017.
- [41] Ron Mokady, Amir Hertz, and Amit H. Bermano. Clipcap: Clip prefix for image captioning, 2021.
- [42] Alex M Lamb, Anirudh Goyal ALIAS PARTH GOYAL, Ying Zhang, Saizheng Zhang, Aaron C Courville, and Yoshua Bengio. Professor forcing: A new algorithm for training recurrent networks. *Advances in neural information processing systems*, 29, 2016.
- [43] Hila Chefer, Shir Gur, and Lior Wolf. Transformer interpretability beyond attention visualization. In *Proceedings of the IEEE/CVF conference on computer vision and pattern recognition*, pages 782–791, 2021.
- [44] Kishore Papineni, Salim Roukos, Todd Ward, and Wei-Jing Zhu. Bleu: a method for automatic evaluation of machine translation. In *Proceedings of the 40th Annual Meeting on Association for Computational Linguistics, ACL '02*, page 311–318, USA, 2002. Association for Computational Linguistics.
- [45] Alon Lavie and Abhaya Agarwal. Meteor: an automatic metric for mt evaluation with high levels of correlation with human judgments. In *Proceedings of the Second Workshop on Statistical Machine Translation, StatMT '07*, page 228–231, USA, 2007. Association for Computational Linguistics.
- [46] Ramakrishna Vedantam, C. Lawrence Zitnick, and Devi Parikh. Cider: Consensus-based image description evaluation. In *Proceedings of the IEEE Conference on Computer Vision and Pattern Recognition (CVPR)*, June 2015.
- [47] Kashyap Chitta, Aditya Prakash, and Andreas Geiger. Neat: Neural attention fields for end-to-end autonomous driving. In *Proceedings of the IEEE/CVF International Conference on Computer Vision*, pages 15793–15803, 2021.

## 7 Supplementary Materials

This supplementary document provides additional details, analyses, and baseline comparisons to support the main paper.

## 8 Dataset Details and Statistics

### 8.1 CARLA Simulator Configuration and Data Collection

We leverage the open-source radar simulator implementation from [24] to generate high-fidelity radar data across diverse driving scenarios. Our data collection spans all daylight conditions including morning, afternoon, evening, dusk, and night, following the scenario distribution from [47]. In total, we collected 861,000 radar-caption frame pairs. The radar sensor is configured to simulate a 77 GHz Texas Instruments cascaded automotive radar system with 86 virtual antennas, providing realistic range-azimuth-Doppler measurements that accurately model real-world automotive radar characteristics.

### 8.2 Actor State Extraction and Filtering

For each simulation frame, we extract the complete state of all actors present in the CARLA world. Actors include vehicles, pedestrians (walkers), and traffic infrastructure elements such as traffic lights and signs. For each actor, we record: unique identifier, 3D location coordinates, transform (pitch, yaw, roll), velocity vector, acceleration vector, traffic light association status, current and ground truth traffic light states, traffic sign type, and applicable speed limits. This comprehensive state representation enables precise spatial reasoning and caption generation.

To focus on perception-relevant objects, we apply distance-based filtering relative to the ego vehicle’s position. Actors located beyond 40 meters from the ego vehicle are excluded from caption generation, as they fall outside the typical sensing and decision-making range for autonomous driving scenarios. For lane-wise classification, we transform actor positions into the ego vehicle’s local coordinate frame where the ego’s forward direction defines the positive x-axis and the left direction defines the positive y-axis. Each vehicle is classified based on its motion direction relative to the ego vehicle using dot products of forward vectors: vehicles are labeled as "same direction" (dot product  $> 0.5$ ), "opposing direction" (dot product  $< -0.5$ ), or "other" (perpendicular or crossing traffic). Within the "same direction" category, lateral offsets determine lane assignment (in-lane, left-lane, or right-lane) using a configurable lane width threshold of 3 meters. Additionally, each vehicle is classified as being ahead, behind, or directly beside the ego vehicle based on the dot product between the ego’s forward vector and the relative position vector to that vehicle. This ego-centric spatial encoding provides the foundation for generating structured, spatially-grounded scene descriptions.

### 8.3 Natural Language Caption Generation

We generate natural language captions from the structured JSON representations using GPT-4.1 mini via the OpenAI API. Rather than relying on fixed templates, we prompt the language model to produce varied descriptions that maintain semantic consistency while introducing lexical diversity. The prompting structure consists of two components: a system prompt that instructs the model to adopt the perspective of a driver describing the scene to a passenger, and a user prompt that provides the JSON data along with detailed key-explanation mappings.

#### 8.3.1 System Prompt

The system prompt establishes the generation style and constraints:

*"You are an expert at describing traffic scenes from the perspective of a driver talking to a passenger. Only output the final caption. Do not include explanations. Also do not use short word forms with apostrophe, use the full expansion of words only."*

This prompt ensures naturalistic descriptions while preventing the model from generating meta-commentary or using contractions, which could introduce inconsistencies during training.

#### 8.3.2 Key-Explanation Mappings

The user prompt includes comprehensive mappings that provide semantic context for each spatial encoding element. These mappings are organized into two categories: distance bins and angular sectors.

##### Distance Bin Mappings:

- 0-10m: "Objects within 0 to 10 meters from the ego vehicle. These are very close and may require immediate attention."
- 10-20m: "Objects within 10 to 20 meters from the ego vehicle. These are close and should be monitored closely."
- 20-30m: "Objects within 20 to 30 meters from the ego vehicle. These are at a moderate distance and should be noted."
- 30-40m: "Objects within 30 to 40 meters from the ego vehicle. These are at a safe distance but still relevant."

#### Angular Sector and Feature Mappings:

- `total_vehicles`: "Total number of vehicles in the distance bin."
- `left_lane_front_side`: "Vehicles in the left adjacent lane ahead of the ego vehicle."
- `left_side`: "Vehicles directly to the left side of the ego vehicle."
- `left_lane_back_side`: "Vehicles in the left adjacent lane behind the ego vehicle."
- `in_lane_front_side`: "Vehicles directly ahead of the ego vehicle in the same lane."
- `in_lane_back_side`: "Vehicles directly behind the ego vehicle in the same lane."
- `right_lane_front_side`: "Vehicles in the right adjacent lane ahead of the ego vehicle."
- `right_side`: "Vehicles directly to the right side of the ego vehicle."
- `right_lane_back_side`: "Vehicles in the right adjacent lane behind the ego vehicle."
- `opposing_lane_front`: "Vehicles in the opposing lane ahead of the ego vehicle."
- `opposing_lane_back`: "Vehicles in the opposing lane behind the ego vehicle."
- `other_lane_front`: "Vehicles in perpendicular or intersecting lanes ahead of the ego vehicle."
- `other_lane_back`: "Vehicles in perpendicular or intersecting lanes behind the ego vehicle."
- `applicable_traffic_signs`: "Traffic signs that are applicable to the ego vehicle."
- `walkers`: "Pedestrians in the scene."

### 8.3.3 Complete Prompt Example

To illustrate the complete prompting structure, consider a scene where the ego vehicle is on a highway with vehicles in multiple lanes. The structured JSON data is first preprocessed: numerical values are converted to word form (e.g., 3 becomes "three"), and keys within each distance bin are randomly shuffled to prevent the model from learning positional biases. The complete user prompt combines the JSON data with the key explanations:

*Here is the JSON data:*

```
{
  "0-10m": {
    "total_vehicles": "three",
    "in_lane_front_side": "one",
    "right_lane_back_side": "two"
  },
  "10-20m": {
    "total_vehicles": "five",
    "right_lane_front_side": "three",
    "in_lane_back_side": "one",
    "right_lane_back_side": "one"
  },
  "20-30m": {
    "total_vehicles": "four",
    "opposing_lane_front": "four"
  },
  "30-40m": {
    "total_vehicles": "two",
    "in_lane_front_side": "one",
```

```

    "right_lane_front_side": "one"
  },
  "applicable_traffic_signs": [],
  "walkers": "zero"
}

```

*Here is the description of every key in the JSON data:*

*Distance Bin - 0-10m: Objects within 0 to 10 meters from the ego vehicle. These are very close and may require immediate attention.*

*[... additional distance bin descriptions ...]*

*- total\_vehicles: Total number of vehicles in the distance bin.*

*- in\_lane\_front\_side: Vehicles directly ahead of the ego vehicle in the same lane.*

*- right\_lane\_back\_side: Vehicles in the right adjacent lane behind the ego vehicle.*

*[... additional key descriptions ...]*

*Given this data, generate natural language sentences describing the scene. Only provide the description. Do not explain how you arrived at it. Include all the fields provided even if it is empty.*

Additionally, we randomly vary whether to include the instruction "Do not add any distance bin numbers" to create captions with and without explicit distance references, further increasing linguistic diversity.

### 8.3.4 Caption Generation Parameters

To enhance caption diversity, we generate multiple caption variants for each radar frame using the following sampling parameters: temperature  $T = 0.5$  to balance creativity with consistency, top-p nucleus sampling with  $p = 0.9$  to constrain the probability mass while allowing varied word choices, maximum token length of 400 to accommodate detailed scene descriptions, and number of samples  $n = 5$  to provide multiple linguistic realizations of the same spatial structure. During training, we randomly sample one caption from this set for each radar frame, ensuring the model learns from diverse expressions of identical spatial configurations while maintaining semantic groundedness.

## 8.4 Hash Vector Encoding Specification

Each scene is encoded as a compact binary hash vector that enables efficient computation of spatial similarity during contrastive learning. The hash structure allocates bits hierarchically to capture both categorical information and spatial occupancy. Traffic sign states receive 4 bits encoding the presence of speed limits, traffic lights, stop signs, and yield signs as binary flags. Pedestrian counts are encoded using 3 bits, allowing representation of 0-7 walkers. The remaining bits encode vehicle presence across the spatial grid defined by distance bins and angular sectors.

For adjacent lane sectors (left-lane, in-lane, right-lane), we allocate 3 bits per sector per distance bin, encoding vehicle counts from 0 to 7. For opposing and perpendicular lane sectors, which typically contain fewer vehicles in structured driving scenarios, we allocate 5 bits per sector per distance bin, allowing counts up to 31. This differentiated bit allocation balances representational capacity with hash compactness. The complete hash vector for a scene with four distance bins totals: 4 (traffic signs) + 3 (walkers) + 12 sectors  $\times$  (3 or 5 bits)  $\times$  4 bins = 55 bits for the 3-bit sectors and 40 bits for the 5-bit sectors, yielding a total of 103 bits per scene. Each distance bin's hash value is constructed by bitwise OR operations that pack vehicle counts into the allocated bit positions, and the final hash list concatenates traffic sign bits, walker bits, and per-bin hash values in sequence.

## 9 Supplementary Videos

We provide supplementary video demonstrations that showcase RadarFM's spatial understanding capabilities during continuous driving sequences. These videos present synchronized multi-modal views of the ego vehicle navigating through diverse traffic scenarios in the CARLA simulator. Each video frame displays: the camera reference view showing the visual scene from the driver's perspective, the corresponding radar range-angle heatmap with attention rollout overlays highlighting spatially relevant regions, ground truth vehicle distributions in radial format across distance bins and angular sectors, and the model's predicted caption describing the scene in natural language. The attention visualizations reveal how the learned representations focus on semantically meaningful spatial structures, while the frame-by-frame caption predictions demonstrate the model's ability to track dynamic changes in traffic configurations as the ego vehicle progresses through intersections, lane changes, and multi-vehicle encounters. These videos provide qualitative evidence of RadarFM's fine-grained spatial reasoning and its capacity to generate accurate, contextually appropriate scene descriptions across varying traffic densities and environmental conditions.